

# Search for Nucleation of Phase Embryos in Binary Alloys by Impurity Atoms

Gary S. Collins, Luke S.-J. Peng, and Matthew O. Zacate

Dept. of Physics, Washington State University, Pullman, WA 99164, USA

Reprint requests to Prof. G. S. C.; Fax: +1-509-335-7816; E-mail: collins@wsu.edu

Z. Naturforsch. **55 a**, 129–133 (2000); received August 25, 1999

*Presented at the XVth International Symposium on Nuclear Quadrupole Interactions, Leipzig, Germany, July 25 - 30, 1999.*

A search was made to detect the possibility that individual impurity atoms in two-phase, binary alloys nucleate embryonic crystals. The alloy system studied was Ni-Al and the impurities were  $^{111}\text{In}$  probe atoms. Local surroundings of the probes characteristic of the crystal phases were detected through quadrupole interactions with  $^{111}\text{Cd}$  daughter nuclei using the method of perturbed angular correlation of gamma rays. Analysis of site fractions of the probes led to two alternative interpretations that could not be distinguished on the basis of the present measurements: 1.)  $^{111}\text{In}$  probes in the two-phase domain between  $\text{Ni}_2\text{Al}_3$  and NiAl segregate to  $\text{Ni}_2\text{Al}_3$  with a segregation energy of about 0.10 eV; or 2.)  $^{111}\text{In}$  probes nucleate embryonic crystals of  $\text{Ni}_2\text{Al}_3$ , with the driving force for nucleation being an attraction between In atoms and Ni vacancies that is known to be strong in NiAl.

**Key words:** Quadrupole Interaction; Phase Embryos; Solute Segregation; Perturbed Angular Correlation; Ni-Al.

Phase separation generally occurs via heterogeneous nucleation and growth. Theoretical treatments focus on extended nucleation sites such as interfaces and dislocations using continuum models [1]. An important issue to raise is what minimum size a nucleation center can have. In particular, can a single impurity atom nucleate and stabilize an embryonic crystal (of nanometer dimensions) of one phase in the range of a two-phase mixture? *A fortiori*, can an embryo be nucleated by an impurity atom within a neighboring single-phase domain? To address these questions, experiments were undertaken using the method of perturbed angular correlation of gamma rays (PAC) to determine lattice locations of probe atoms in Ni-Al alloys. Lattice sites were determined through characteristic quadrupole interactions of  $^{111}\text{In}/\text{Cd}$  probes in the intermetallic phases  $\text{Ni}_2\text{Al}_3$  and NiAl. Studied compositions included the stoichiometric compositions, 40 and 50 at.-% Ni, respectively, and a two-phase region in between phase boundaries at low temperature at 42.2 to 45.2 at.-% Ni [2]. Samples were prepared by arc-melting the constituent elements and a dried drop of carrier-free  $^{111}\text{In}$  radioactivity together, followed

by annealing for about one hour in the range 800 - 1200 °C and slow cooling in furnace to room temperature. X-ray analysis of some samples confirmed the presence of only the  $\text{Ni}_2\text{Al}_3$  and NiAl phases. In all measurements the fractional concentration of  $^{111}\text{In}$  probes was below  $10^{-8}$ . PAC measurements were made as described in [3].

Since the quadrupole interaction is very short ranged, the signal of a probe at the center of a metallic crystal of nanometer dimensions is not expected to differ from that of a macroscopic crystal. Our basic idea here is to measure site fractions of probes in the two phases and to compare the observed site fractions with volume fractions of the two phases, given in terms of the sample's composition and phase boundaries by the lever rule. For a composition  $x$  between phase boundaries at  $x_1$  and  $x_2$ , the lever rule predicts the volume fraction  $f_1^{\text{vol}}$  of phase 1 to be

$$f_1^{\text{vol}} = \frac{x_2 - x}{x_2 - x_1}. \quad (1)$$

The site fraction of probes in phase 1 will equal the volume fraction as long as probes neither nucleate

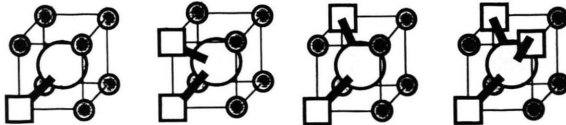


Fig. 1. Vacancy complexes with  $\text{In}_{\text{Al}}$  probe atoms in  $\text{NiAl}$  detected by PAC. The probe atom (large circle) is surrounded in the perfect lattice by eight Ni atoms (small circles) in the first neighbor shell. From left to right are a monovacancy (1V) complex, two distinct divacancy complexes, 2V(a) and 2V(b), and a trivacancy complex.

embryonic crystals nor segregate to one of the phases. When there is segregation, it can be shown that the site fraction of probes in phase 1 is given by

$$f_1 = \left( 1 + A \exp(-E_{\text{seg}}/k_{\text{B}}T) \frac{x - x_1}{x_2 - x} \right)^{-1}, \quad (2)$$

in which  $E_{\text{seg}}$  is the segregation energy and  $A$  is a prefactor accounting for entropy factors and different numbers of sites in the two phases. A method for distinguishing between segregation phenomena and nucleation is described further below.

The In probes in both alloys are assumed to come to rest on Al lattice-sites for the following reasons. 1.) An oversized In impurity fits better in the more spacious Al-sites. 2.) The solid solubility limit for In in Ni is about 5 at.% but only at the ppm level in Al, suggesting that Ni-sites (surrounded by Al-atoms) are energetically disfavored. 3.) The B2 (CsCl) phase of  $\text{NiAl}$  extends down to 45.2 at.% Ni by incorporation of Ni-vacancies ( $\text{V}_{\text{Ni}}$ ) rather than of Al-antisite atoms ( $\text{Al}_{\text{Ni}}$ ). It is expected that  $\text{In}_{\text{Ni}}$  impurities would have an even higher formation energy than unobserved  $\text{Al}_{\text{Ni}}$  defects.

$\text{NiAl}$  has a unique Al site. The related  $\text{Ni}_2\text{Al}_3$  structure is derivable from the B2 structure by condensation of Ni-vacancies ( $\text{V}_{\text{Ni}}$ ) on every third 111-plane of Ni-atoms, emptying the planes [2]. Removing every third plane results in two inequivalent Al-sites: 2/3 of the Al-sites have one empty and one filled adjacent Ni-plane (site A) and 1/3 have two filled adjacent Ni-planes (site B). Ignoring lattice relaxations following removal of the Ni-planes, it can be readily shown that the first neighbor shells of  $\text{In}_{\text{Al}}$  probes in site A will have three  $\text{V}_{\text{Ni}}$  in a 111-plane while site B probes will have two  $\text{V}_{\text{Ni}}$  on opposite sides. Thus, the magnitudes of the expected quadrupole interactions are large, as observed.

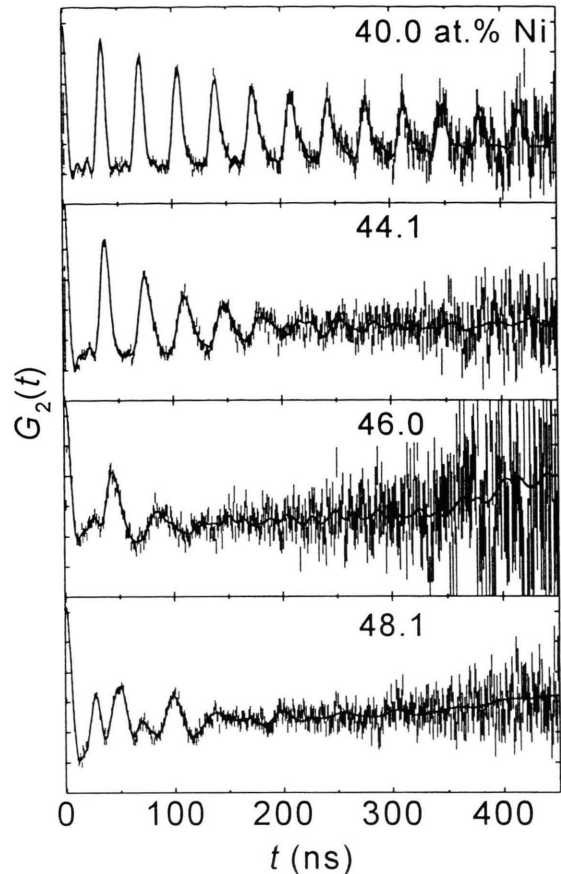


Fig. 2. PAC spectra of Ni-Al alloys at the indicated compositions. The vertical range of each spectrum is from  $-0.20$  to  $+1.10$ .

Site fractions were determined from PAC signal amplitudes for probe atoms in the various phases. For  $\text{NiAl}$ , observed signals have been attributed to local environments of probe atoms having 0 - 2 near-neighbor (nn) vacancies on the Ni-sublattice ( $\text{V}_{\text{Ni}}$ ) [4]. A new signal is reported here that is attributed to 3 nn  $\text{V}_{\text{Ni}}$ , in analogy with a site detected in  $\text{FeAl}$  [5]. Diagrams of the vacancy complexes are shown in Figure 1.

For  $\text{Ni}_2\text{Al}_3$ , two signals were measured that are consistent with In probes on the two inequivalent, defect-free Al-sites, both having electric field-gradient (efg) asymmetry parameters  $\eta \equiv |(V_{xx} - V_{yy})/V_{zz}|$  equal to zero. A third signal prominent in the range 42 - 46 at.% Ni, is attributed to point defects. Quadrupole interaction parameters measured at room temperature, including the fundamental measured frequency,  $\omega_1$ , are listed in Table 1. The cou-

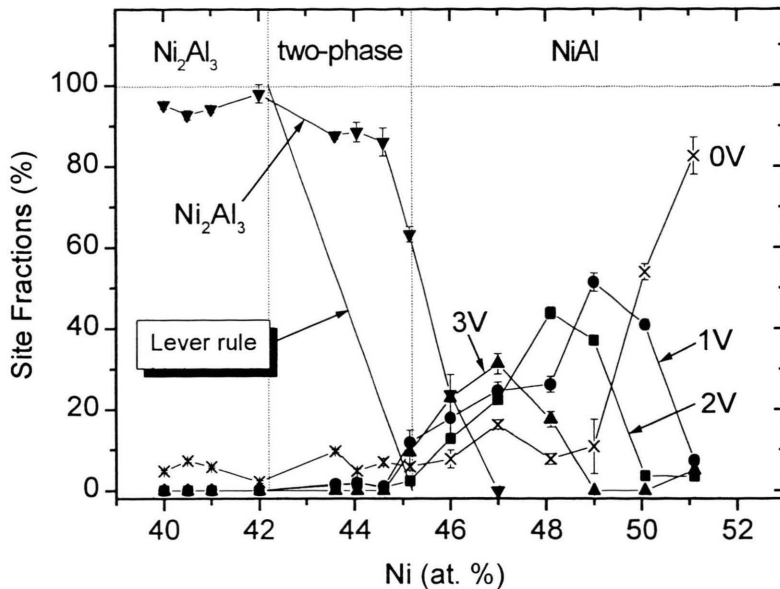


Fig. 3. Site fractions of In impurities in Ni-Al alloys. For the NiAl phase, fractions are shown for probes having 0, 1, 2 or 3 near-neighbor Ni-vacancies. For the  $\text{Ni}_2\text{Al}_3$  phase, the sum of fractions for all its sites is shown.

Table 1. Quadrupole interaction parameters for  $^{111}\text{In}/\text{Cd}$  probe sites in Ni-Al alloys.

Phase	Site Description	$\omega_1$ (Mrad/s)	$\eta$	Ref.
NiAl	Defect-free	0 - 20	—	[4, 7]
	1 $\text{V}_{\text{Ni}}$	125(2) <sup>a</sup>	0.00(6)	[4, 7]
	2 $\text{V}_{\text{Ni}}$ (configuration a)	187(1)	0.64(1)	[4, 7]
	2 $\text{V}_{\text{Ni}}$ (configuration b)	222(2)	0.89(1)	[4, 7]
	3 $\text{V}_{\text{Ni}}$	140(3)	0.0(1)	this work
$\text{Ni}_2\text{Al}_3$	A ( $\text{In}_{\text{Al}}$ next to empty 111 Ni-plane)	175(2)	0.0(1)	this work
	B ( $\text{In}_{\text{Al}}$ not next to empty 111 Ni-plane)	181(1)	0.00(6)	this work
	X (defect-associated site)	168(3)	0.1(1)	this work

<sup>a</sup> For the 1V signal we used 125 Mrad/s in the analysis here as more appropriate for Ni-poor compositions than the value 128 Mrad/s cited in the references.

pling frequency  $\nu_Q = eQV_{zz}/\hbar$  can be calculated algebraically from  $\omega_1$  and  $\eta$  as described in [6]. The defect-free signal listed in the table also includes low-frequency components (< 20 Mrad/s) attributed to distant defects.

For  $\text{Ni}_2\text{Al}_3$ , signals were attributed to defect-free sites A and B as indicated in the table because the 181 Mrad/s signal generally had a smaller site fraction and, in addition, a smaller amount of inhomogeneous broadening due to distant defects. It is believed that inhomogeneous broadening should be greater for probes in site A, next to empty Ni-planes, because of the presence of random intercalating Ni-atom defects. The site fraction of the 168 Mrad/s signal, site X,

increases with Ni content, suggesting that it is associated with Ni-atom defects intercalated in adjacent empty planes. However, a precise configuration can not be stated.

Representative PAC spectra are shown in Figure 2. The spectrum for the 40% sample is characteristic of  $\text{Ni}_2\text{Al}_3$  and is dominated by the 181 and 175 Mrad/s signals. The apparent attenuation is due to the closeness in frequencies and not to inhomogeneous broadening. The spectrum for the 44% sample exhibits increased damping due to inhomogeneous broadening. This is attributed to point defects such as Ni-atoms intercalating in the empty Ni-planes. The spectrum for the 46% sample was fitted to a superposition of many signals of both  $\text{Ni}_2\text{Al}_3$  and NiAl phases. Finally, the spectrum for the 48% sample was fitted with a superposition of signals for the NiAl phase.

Site fractions fitted to these and other spectra are shown as a function of composition in Figure 3. For simplicity, the figure shows only sums of site fractions of the two 2V configurations in the NiAl phase and of the three configurations in the  $\text{Ni}_2\text{Al}_3$  phase (termed 23-phase below). Experimental site fractions have been normalized to 100%. Also shown in Fig. 3 are the phase boundaries at 42.2 and 45.2 at.% Ni, and a sloping straight line that gives the predicted trend of the volume fraction of the 23-phase according to the lever rule. As can be seen, the observed 23-site-fraction is clearly in excess of the expected 23-volume-fraction, meaning that In probes have a

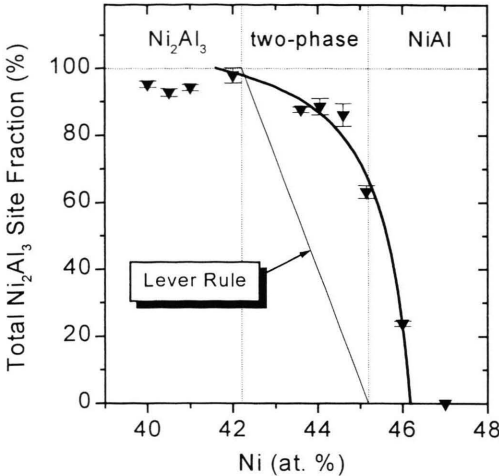


Fig. 4. Site fraction of probes in the  $\text{Ni}_2\text{Al}_3$  phase as a function of composition. The curve is from a fit of the data to (2) under the assumption that the probes are segregating to that phase.

greatly enhanced probability of being found in the 23-phase. Two alternative explanations are now evaluated: 1.) In segregates to the 23-phase. 2.) In atoms nucleate small embryonic crystals of the 23-phase.

Supposing the trends are due to segregation, the site fractions of the 23-phase shown in Fig. 3 were fitted as a function of composition using (2), with the fitted curve shown in Figure 4. A rough estimate of  $E_{\text{seg}}$  can be obtained by assuming that, during cooling of the samples to room temperature in furnace, equilibrium was maintained down to a temperature  $T^*$  below which atomic mobility ceased. For NiAl, the value  $T^* = 620(50)$  K was previously determined by PAC for furnace coolings under similar conditions [8]. Results of the fits are  $x_1 = 41.6(1.6)$  at. % Ni,  $x_2 = 46.2(1)$  at. % Ni, and  $A \exp(-E_{\text{seg}}/k_B T^*) = 0.14(8)$ . Using  $A = 1$  and  $T^* = 620(50)$  K yields  $E_{\text{seg}} = 0.10(3)$  eV. The fitted phase boundary  $x_2 = 46.2$  at. % Ni disagrees with the literature value of 45.2%. If the disagreement were real, it would imply that In probes nucleate  $\text{Ni}_2\text{Al}_3$  embryonic crystals at a composition within the single-phase NiAl domain. However, there is enough uncertainty in our analysis and in the published phase diagram that the disagreement can not be considered conclusive. The relatively small segregation energy obtained appears to be of plausible magnitude, although no value is known to us for comparison. Thus, segregation of In to the 23-phase can explain the observed site fractions in an acceptable way.

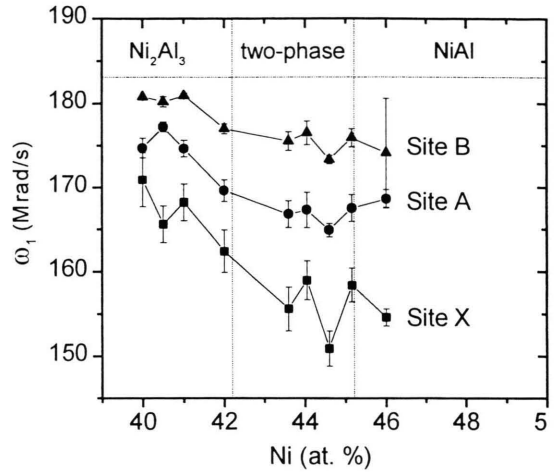


Fig. 5. Composition dependence of quadrupole interaction frequencies of the three signals detected in the  $\text{Ni}_2\text{Al}_3$  phase.

Is there evidence for nucleation? A driving force for nucleation in this system of alloy and impurity could be a strong binding between In solutes and Ni-vacancies, known to be about 0.20 eV [9]. We suppose that embryonic crystals nucleating on impurities may have a variable composition that depends on the overall composition of the alloy. On the other hand, normal two-phase mixtures should have constant compositions equal to those at the phase boundaries. Therefore, we examined whether there was evidence for a varying composition through quadrupole interaction parameters. In Fig. 5 is shown the composition dependence of the quadrupole interaction frequencies for the three sites in the 23-phase. The variation visible in the one-phase domain between 40 and 42 % Ni is attributed to a changing axial ratio and unit cell volume [2]. In the two-phase region between 42 and 45 % Ni, however, little evidence can be seen of any composition dependence. Therefore, no conclusion can be drawn that segregation is not at the origin of the enhanced site fraction for the 23-phase. Similarly, the amount of inhomogeneous broadening of signals in the two-phase domain was not observed to change.

In summary, it was not possible in the present work to demonstrate that dilute In impurities nucleate embryonic crystals of a phase. An alternative phenomenon, solute segregation, could not be ruled out and can well explain the observed trends. Additional PAC measurements in progress will seek to differentiate between embryo formation and segregation through measurements at elevated temperature.

Another method that may be able to detect embryos such as are proposed here and, in addition, determine their size is small angle x-ray scattering.

This work was supported in part by the National Science Foundation under grant DMR 96-12306 (metals program).

- [1] The Theory of Transformations in Metals and Alloys, J. W. Christian, 2<sup>nd</sup> ed., Pergamon Press, Oxford 1975.
- [2] A. Taylor and N. J. Doyle, *J. Appl. Cryst.* **5**, 201 (1972).
- [3] G. S. Collins, S. L. Shropshire, and J. Fan, *Hyperfine Interactions* **62**, 1 (1990).
- [4] J. Fan and G. S. Collins, *Hyperfine Interactions* **60**, 255 (1990). See also Ref. [3].
- [5] Gary S. Collins, Luke S.-J. Peng, and Mingzhong Wei, in *High-temperature Ordered Intermetallic Alloys VIII*, eds. E. P. George, M. Mills, and M. Yamaguchi, *Materials Research Society Symposium Proceedings* **552**, 191 (1999).
- [6] D. Wegner, *Hyperfine Interactions* **23**, 179 (1985). Note that the first factor in parentheses in (5b) should be  $(1 - \eta^2)$ .
- [7] Gary S. Collins, Praveen Sinha and M. Wei, *Hyperfine Interactions* **C1**, 380 (1996).
- [8] Bin Bai, Ph. D. dissertation, Washington State University, 1998 (unpublished).
- [9] Bin Bai and Gary S. Collins, in *High-temperature Ordered Intermetallic Alloys VIII*, eds. E. P. George, M. Mills, and M. Yamaguchi, *Materials Research Society Symposium Proceedings* **552**, 541 (1999).